

Electronic Supplementary Information for

Porous Ionic/Molecular Crystal Composed of Highly Symmetric Magnetic Clusters

Xiao-Ning Cheng,^{a,b} Wei Xue,^a Jian-Bin Lin,^a and Xiao-Ming Chen^{*a}

^a *MOE Laboratory of Bioinorganic and Synthetic Chemistry, School of Chemistry & Chemical Engineering, Sun Yat-Sen University, Guangzhou 510275, China.*

^b *Instrumental Analysis and Research Center, Sun Yat-Sen University, Guangzhou 510275, China.*

Materials and Physical Measurements

All solvents and starting materials for synthesis were purchased commercially, and were used as received. Powder X-ray diffraction (PXRD) data were recorded on a Bruker D8 Advance diffractometer. FT-IR (KBr pellet) spectra were recorded from KBr pellets in the range of 400-4000 cm^{-1} on a Bruker TENSOR 27 FT-IR spectrometer. Elemental analysis (C, H, N) was performed on a Perkin-Elmer 240 elemental analyzer. Both ac and dc magnetic data were collected using a Quantum Design MPMS XL-7-SQUID magnetometer on phase-pure samples from crushed single crystals. The powder samples of these compounds were embedded in grease to avoid any field-induced crystal reorientation. The magnetic data were corrected for the diamagnetic contribution calculated from Pascal constants.

X-Ray Crystallography. The diffraction data were collected on a Bruker Smart Apex CCD diffractometer with graphite monochromated Mo-K α radiation ($\lambda = 0.71073 \text{ \AA}$) at 293 K. The absorption correction was applied by SADABS. The structure was solved by direct methods and refined with full-matrix least-squares technique using SHELXTL.¹ All non-hydrogen atoms were refined with anisotropic displacement parameters except the solvent molecules and nitrate anions. The aqua hydrogen atoms were located from the difference Fourier map at the final states of refinements.

Due to no strong interaction with the host clusters, the nitrate anion and lattice water molecules having low occupancy are highly disorder, so these atoms cannot be refined anisotropically. The occupancies of the anion and guest water molecules are determined by combination of the results from IR, TGA, and EA, as well as charge balance consideration. The alerts of A and B in checkcif report are caused by the disorder.

Ref 1. *SHELXTL 6.10*, Bruker Analytical Instrumentation, Madison, Wisconsin, USA, 2000.

Synthesis of 1·g.

Solvothermal reaction of a mixture of 8-hydroxyquinoline (0.070 g, 0.5 mmol), $\text{Co}(\text{NO}_3)_2 \cdot 6\text{H}_2\text{O}$ (0.150 g, 0.5 mmol), triethylamine (0.25 mL), and methanol (10 mL) in a 15-mL Teflon-lined bomb at 160°C for 3 days afforded dark-green octahedral crystals (yield *ca.* 61%). Anal. Calcd (%) for $\text{C}_{108}\text{H}_{104}\text{Co}_8\text{N}_{14}\text{O}_{35}$: C, 49.67; H, 3.94; N, 7.51. Found: C, 49.7; H, 4.00; N, 7.39.

The elemental analyses of **1**·g found: C, 49.7; H, 4.00; N, 7.39%. These data confirm that there are two nitrates and sixteen guest water molecules for per Co₈ unit of **1**·g with calculated: C, 49.67; H, 3.94; N, 7.51%.

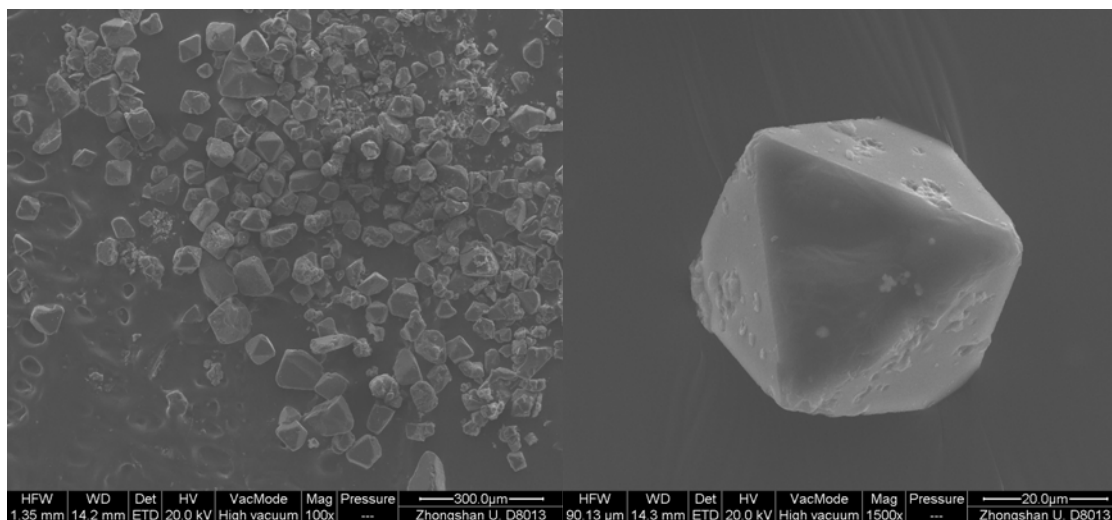


Figure S1. SEM images of the crystals of **1**·g.

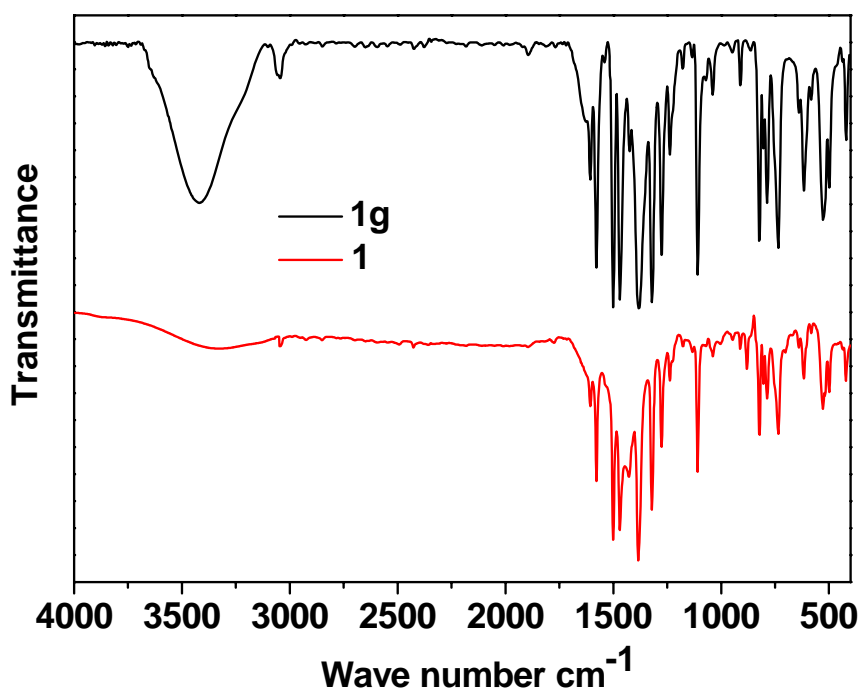


Figure S2. Infrared spectrum of **1**·g and **1**. The characteristic infrared peaks of nitrate anion (at 1382 cm⁻¹) is observed, which confirms the existence of nitrate in **1**·g.

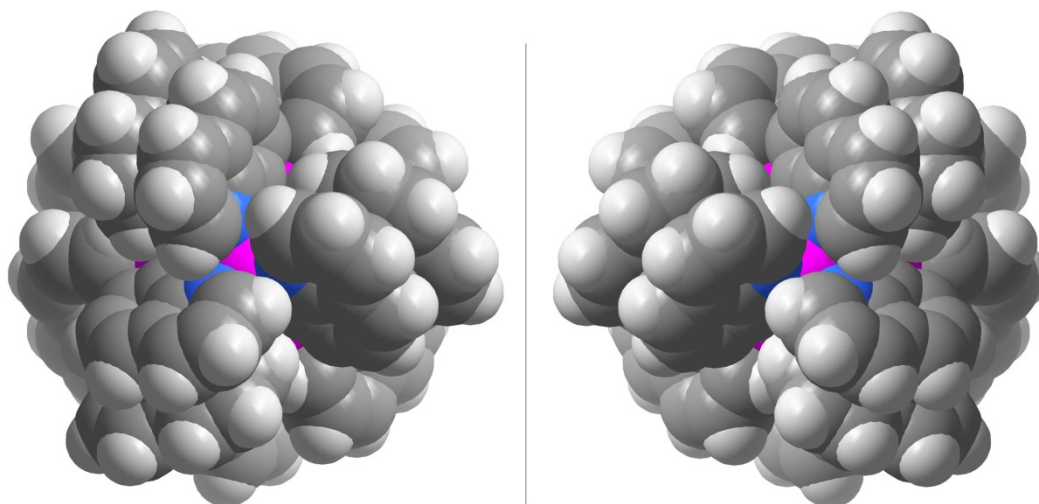


Figure S3. In the same Co₈ cluster, four *fac*-{CoQ₃}⁻ moieties are either all in Δ or all in Λ modes, furnishing Co₈ clusters in different chiralities, which are further packed into a centrosymmetric 3D structure.

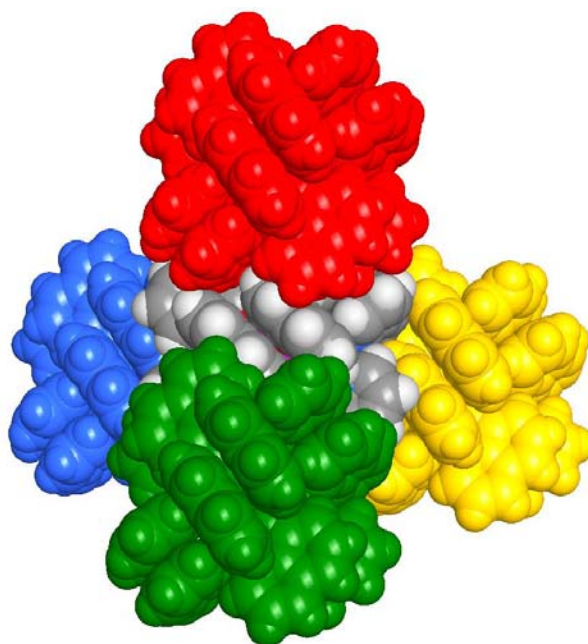


Figure S4. The tetrahedral packing fashion of Co₈ cations.

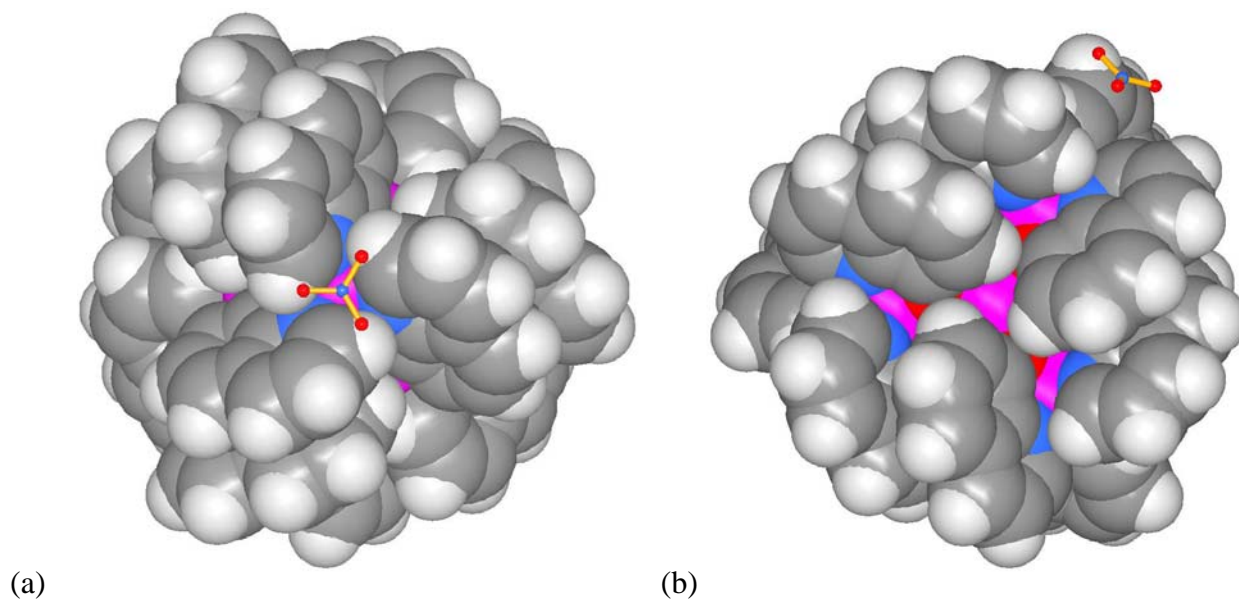


Figure S5. Views of the position of nitrate related to the Co_8 cation along the $[1\ 1\ 1]$ (a) and $[1\ 1\ -1]$ (b) directions. The best crystallographic model suggested that two nitrates are located at the $[1\ 1\ 1]$ and other three equivalent 3-fold axes (i.e. each position has half occupancy) near the surface of the Co_8 cluster (a). The Co_8 cations use the other four 3-fold axes ($[1\ 1\ -1]$ and equivalents) to interact with four neighbors and extend to a 3D diamondoid supramolecular network (b). The shortest cation-anion contact is $\text{C-H}\cdots\text{O}$ ($\text{C}\cdots\text{O}$ 3.55 Å, $\text{C-H}\cdots\text{O}$ 113.2°).

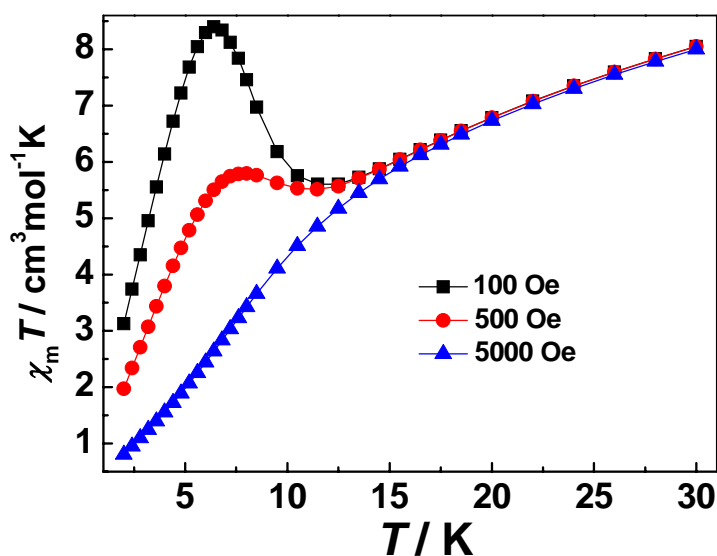


Figure S6. Field-cooled magnetization curves for **1-g** at different fields.

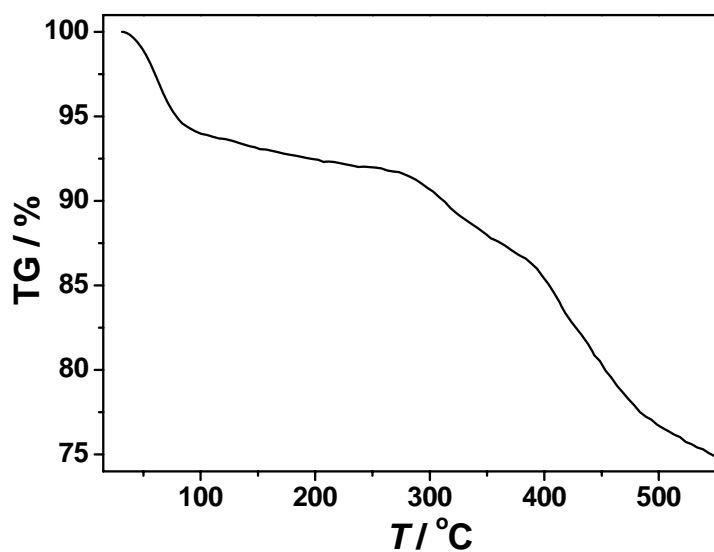


Figure S7. Thermogravimetry of **1·g** in N_2 atmosphere with the heating rate of $5^\circ\text{C}/\text{min}$.

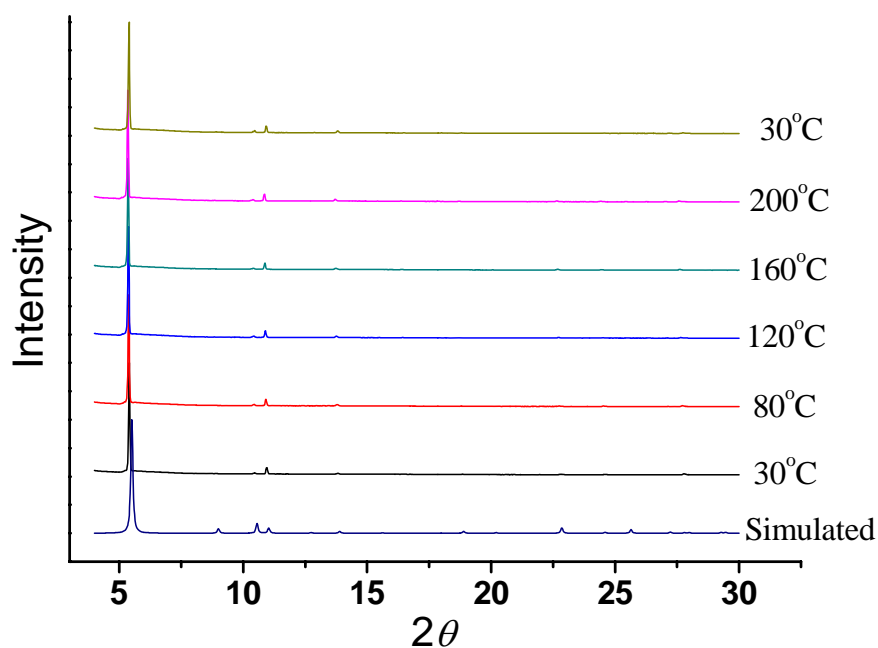


Figure S8. Temperature-dependent X-ray powder diffraction and simulated patterns of **1·g**. The heating rate between the diffraction measurements was $5^\circ\text{C}/\text{min}$, and the temperature was kept for 10 min for each diffraction measurement. The measurements were performed from 30°C to 200°C , then the sample was cooled down to take the measurement at 30°C again.

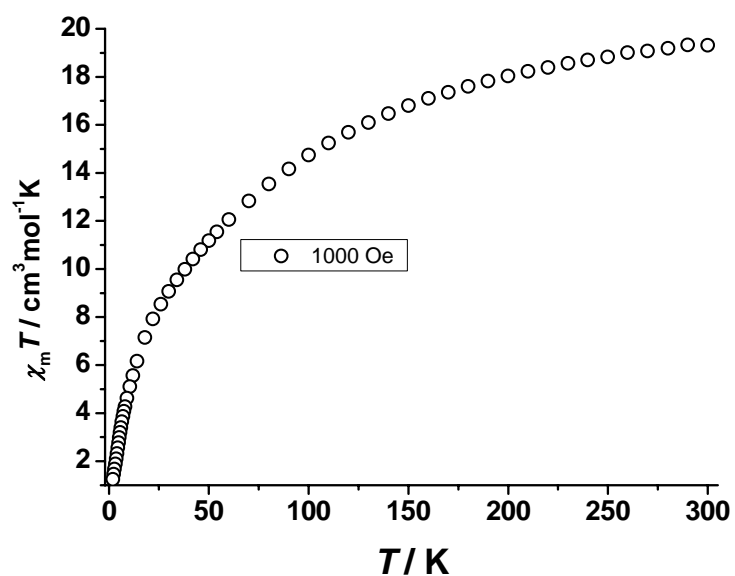


Figure S9. The temperature-dependent susceptibilities of **1** at 1000 Oe.

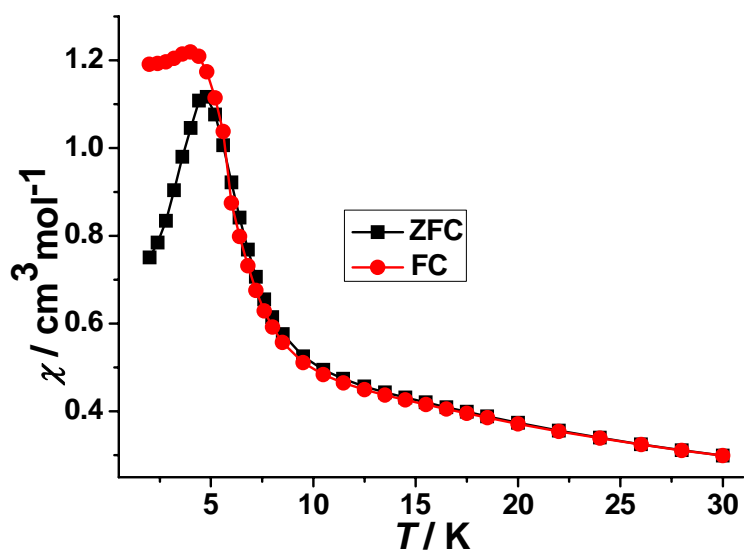


Figure S10. FC and ZFC magnetizations at 20 Oe for **1**.

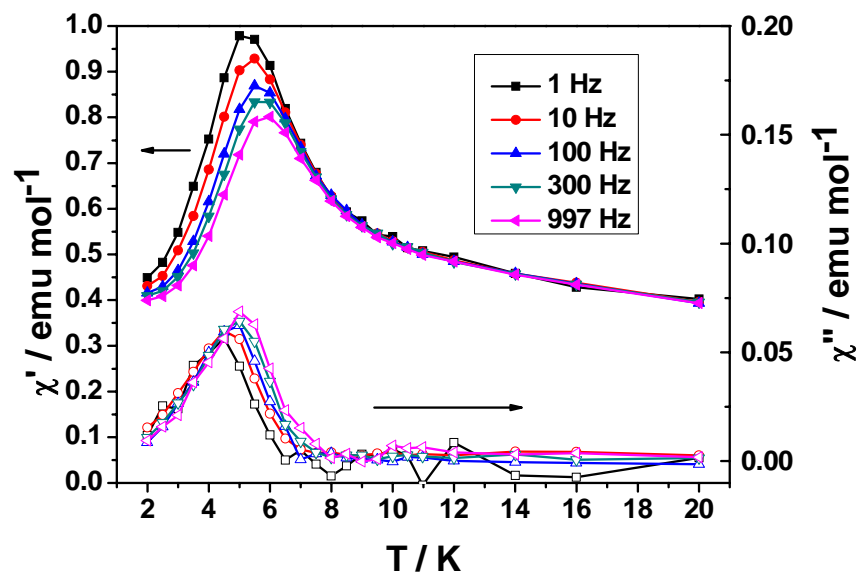


Figure S11. Temperature dependence of ac susceptibility at various frequencies for **1**.

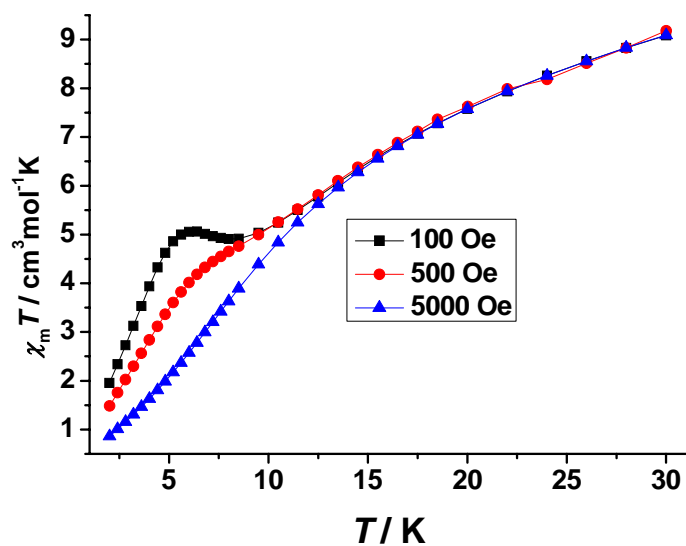


Figure S12. Field-cooled magnetization curves for **1** at different fields.

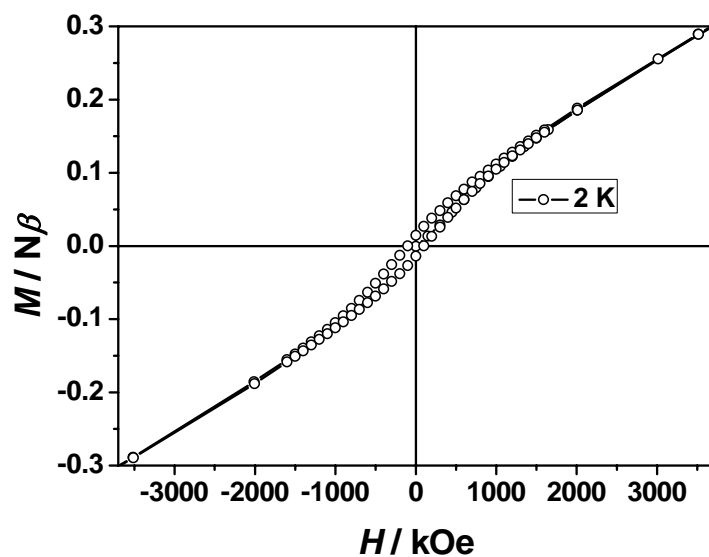


Figure S13. Hysteresis curve for **1** at 2 K.

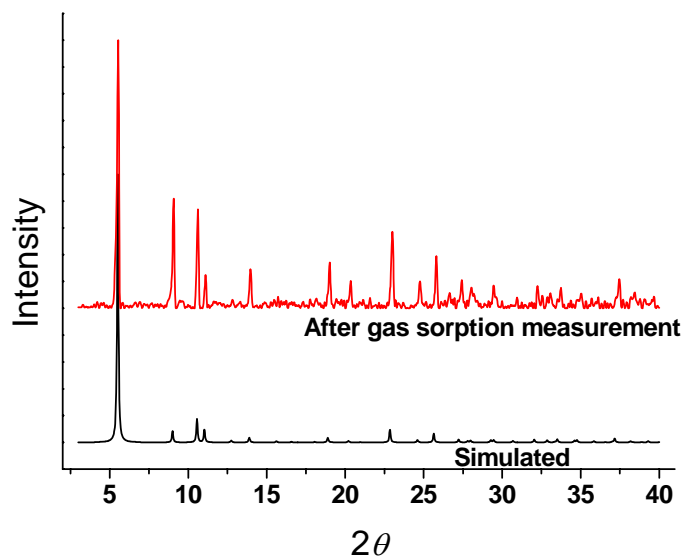


Figure S14. XRPD pattern of **1** after gas sorption measurement resemble the simulated one from **1**·g.

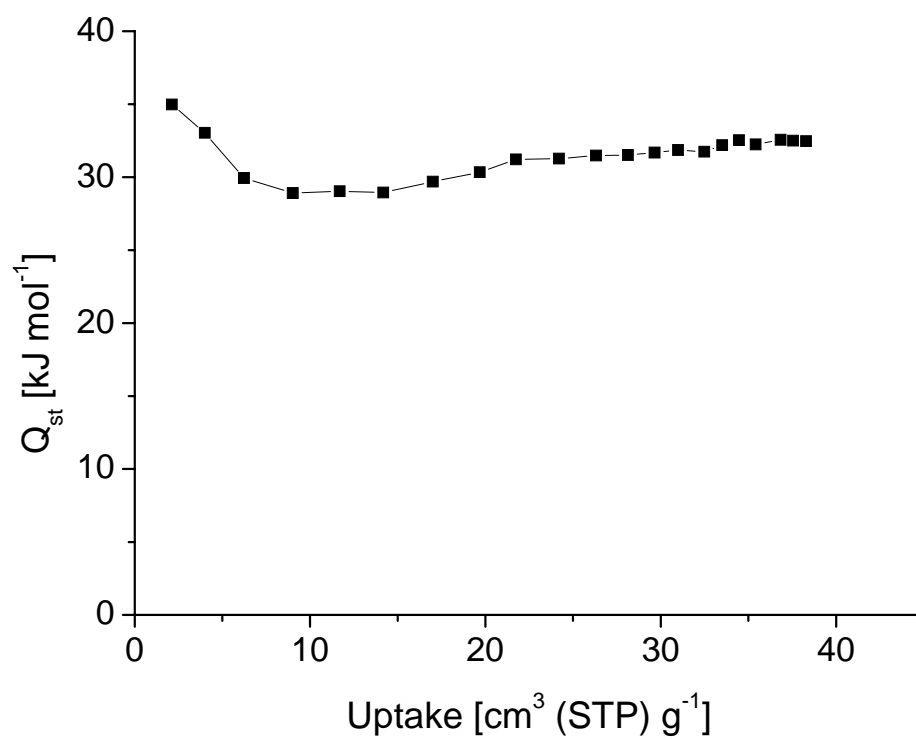
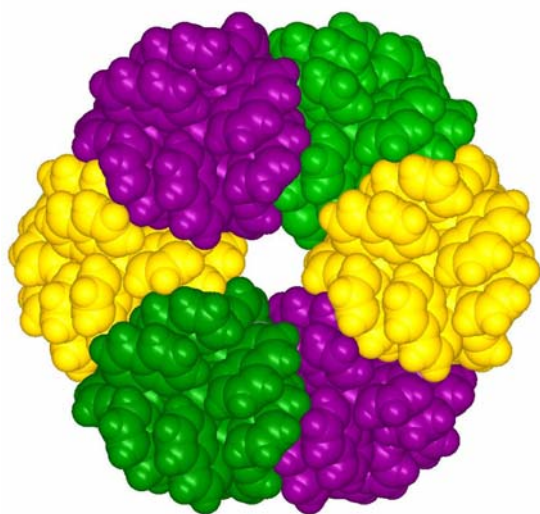
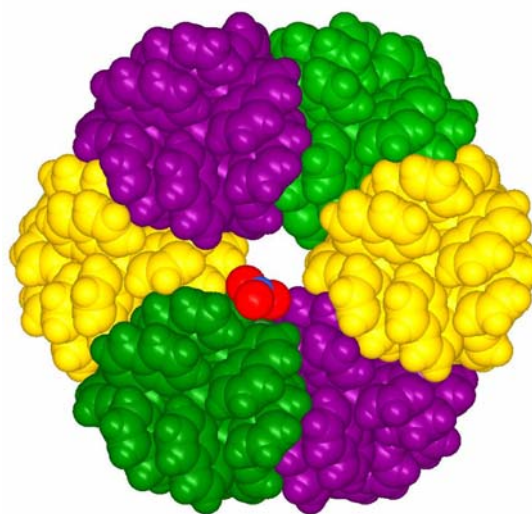


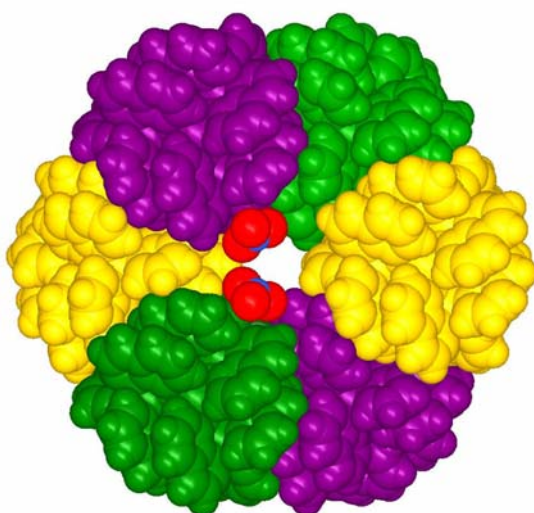
Figure S15. Adsorption isosteric heats of CO₂ for **1** calculated by Clausius-Clapeyron equation.



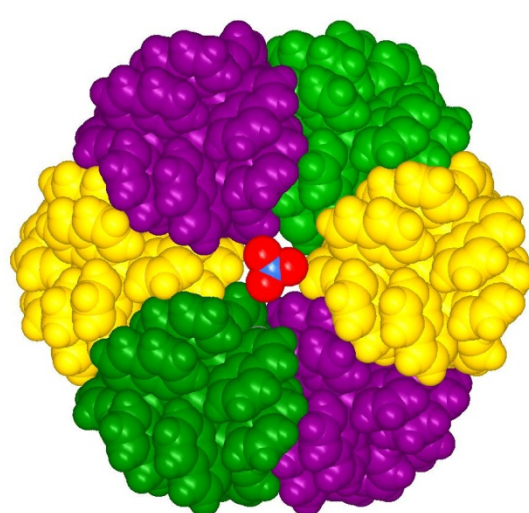
(a)



(b)



(c)



(d)

Figure S16. Views of the nitrate location-dependent apertures (along a 3-fold axis). When nitrate is omitted, the cavities are connected by hexagonal apertures with $d = 4.3 \text{ \AA}$ (a). According to the static structural model from crystallography, each aperture is surrounded by either one (b) or two (c) nitrates, narrowing the aperture to irregular shapes. However, the highly disordered nitrates may not necessarily always locate at the fixed positions such as (b) and (c). They may also adopt other positions to completely open (a) or close (d) the apertures.